Root-Specific *CLE19* Overexpression and the *sol1/2* Suppressors Implicate a CLV-like Pathway in the Control of *Arabidopsis* Root Meristem Maintenance

Eva Casamitjana-Martínez,[1] Hugo F. Hofhuis,[1]
Jian Xu,[1] Chun-Ming Liu,[2] Renze Heidstra,[1]
and Ben Scheres[1,*]
[1]Developmental Genetics
Utrecht University
Padualaan 8
3584 CH Utrecht
[2]Plant Research International
B.V.
P.O. Box 16
6700 AA Wageningen
The Netherlands

Summary

In the *Arabidopsis* shoot apical meristem, an organizing center signals in a non-cell-autonomous manner to specify the overlying stem cells [1, 2]. Stem cells express the small, secreted protein CLAVATA3 (CLV3; [3]) that activates the CLV1-CLV2 receptor complex, which negatively controls the size of the organizing center [4–6]. Consistently, *CLV3* overexpression restricts shoot meristem size [6]. The root meristem also contains a stem cell organizer, and here we show that localized overexpression in roots of *CLE19*, encoding a CLV3 homolog, restricts the size of the root meristem. This suggests that CLE19 acts by overactivating an endogenous CLV-like pathway involved in root meristem maintenance. Surprisingly, CLE19 restricts meristem size without directly interfering with organizer and stem cell specification. We isolated mutations in two loci, *SOL1* and *SOL2*, which suppress the *CLE19* overexpression phenotype. *sol2* plants display floral phenotypes reminiscent of *clv* weak alleles; these phenotypes suggest that components of a CLV pathway are shared in roots and shoots. *SOL1* encodes a putative Zn_{2+}-carboxypeptidase, which may be involved in ligand processing.

Results and Discussion

In the *Arabidopsis* root meristem, the stem cells or initials surround a group of mitotically less active cells, the quiescent center (QC) [7]. Laser ablation experiments suggested that the QC inhibits the differentiation of surrounding stem cells by short-range non-cell-autonomous signals [8]. Consistently, the putative transcription factors *SCR* and *SHR*, which are involved in the specification of the QC, are required to maintain stem cell fate in the immediately surrounding cells [9]. Daughters of stem cells no longer touch the QC, and they differentiate according to positional cues [10]. Since the stem cell organizing capacity of the QC in roots seems equivalent to the role of the stem cell organizer in the SAM, we

investigated whether a CLV-like pathway might operate in roots to control root meristem maintenance.

Overexpression of *CLE19* in Root Meristems Affects Root Meristem Maintenance

CLE19 is a small potentially secreted protein belonging to the CLE family, of which *CLV3* is the founding member [11]. *CLE19* expression has been reported in leaves, flowers, siliques, and pollen [12], and by using Reverse Transcriptase (RT)-PCR, we could detect low levels of the *CLE19* transcript in seedling roots (Figure 1B, WT). Ectopic expression of the *Brassica napus CLE19* ortholog *LIGAND LIKE PROTEIN1* (*BnLLP1*) under the *35SCaMV* promoter causes root meristem termination, among other phenotypes, in *Arabidopsis* (C.-M.L., unpublished data). Recently, it has been reported that high levels of CLV3 and CLE40 also reduce root meristem activity, while *clv3* and *cle40* mutants have no root meristem maintenance phenotype [13, 14]. Thus, the root meristem responds to overexpression of several CLE proteins, indicating that either a promiscuous CLV response pathway is present in the root or that *CLE* expression in other regions of the plant indirectly causes root meristem reduction.

To address whether *CLE* expression specifically in the root meristem can induce the reduction of root size, we expressed the *Arabidopsis CLE19* under the control of the *RCH1* promoter, which confers high and specific expression in the root meristem (Figure 1F). The *BnLLP1* cDNA is smaller than the predicted *CLE19* (C.-M.L., unpublished results; [11]); thus, we used the *CLE19* coding sequence starting at the second methionine, which corresponds to the *BnLLP1* cDNA region. We used the GAL4VP16-*UAS* (upstream activating sequence) transactivation system, whereby the *RCH1* promoter drives expression of GAL4VP16, which in turn promotes the transcription of *ERGFP* by binding to its *UAS* promoter element (*RCH1::GAL4VP16 UAS::ER-GFP* construct, renamed *RCH1-ERGFP*). *CLE19* under the control of the *UAS* element was then cloned into this vector, resulting in *RCH1::GAL4VP16 UAS::ER-GFP UAS::CLE19*, renamed *RCH1-CLE19* hereafter for simplicity (Figure 1A). *Arabidopsis* plants of ecotype Utr were transformed with the *RCH1-CLE19* vector, and transgenic plants were selected for root GFP expression.

A total of 23 independent lines carrying the transgene showed similar "short root" phenotypes. The initial T2 lines tested carried multiple copies of the transgene, and we selected a homozygous, single insertion *RCH1-CLE19* transgenic line in the T3 ("*RCH1-CLE19* transgenic plants" always refers to this single insertion line hereafter). While the *CLE19* transcript is present at high levels in seedling roots of *RCH1-CLE19* transgenic plants (Figure 1B, *RCH1-CLE19*), overexpression of *CLE19* in the root meristem causes progressive loss of meristematic cells in a dose-dependent manner. Hemizygous plants, which were distinguished by lower GFP expression in the root meristem, behave as wild-type
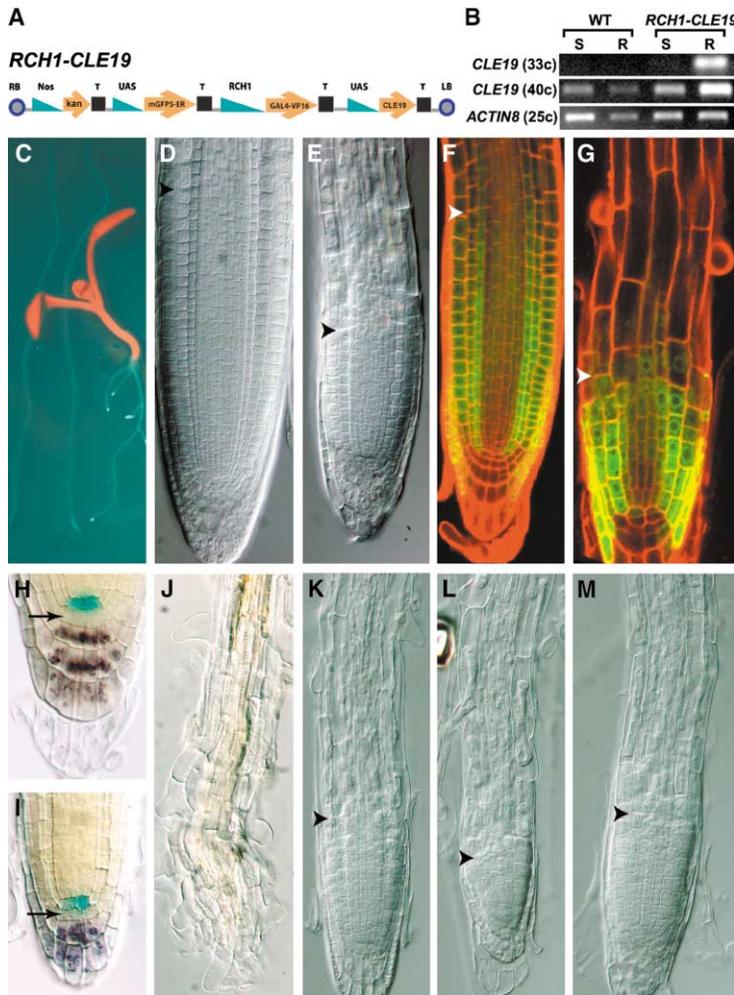
*Correspondence: b.scheres@bio.uu.nl

Figure 1. Overexpression of *CLE19* in the Root Meristem Reduces Meristem Size without Affecting QC Specification and Stem Cell Status

(A) The RCH1-CLE19 construct (promoters in green; coding regions in orange).

(B) RT-PCR using total RNA from shoots (S, hypocotyl, cotyledons, and SAM) and roots (R) of 6-day-old WT and *RCH1-CLE19* transgenic seedlings. Specific primers for *CLE19* (upper panels) and *ACTIN8* (lower panel) were used. The numbers in between the brackets indicate the cycle numbers per reaction.

(C) One-week-old seedling roots viewed under a GFP binocular. From left to right: WT, hemizygous *RCH1-CLE19*, and homozygous *RCH1-CLE19*.

(D and E) Nomarski images showing the root meristem boundary (arrowhead) of a 4-day-old WT and an *RCH1-CLE19* transgenic root.

(F and G) Confocal images showing the root meristem boundary (arrowhead) of 1-week-old *RCH1-ERGFP* and *RCH1-CLE19* transgenic roots.

(H and I) Double labeling of QC and differentiated columella cells visualized by the QC25 marker and amyloplast staining in 1-week-old WT and *RCH1-CLE19* transgenic roots. The columella initials (arrow) do not show signs of differentiation.

(J) The QC25 marker is no longer expressed in a 14-day-old, terminated *RCH1-CLE19* transgenic root.

(K–M) Nomarski images reveal the root meristem boundary (arrowhead) in 6-day-old roots from homozygous *RCH1-CLE19*, double homozygous *RCH1-CLE19 shr-1*, and homozygous *shr-1* seedlings.

(WT) roots, while homozygous *RCH1-CLE19* transgenic plants have short roots with high GFP expression (Figures 1C). These phenotypes indicate that two doses of *RCH1-CLE19* are required to affect root growth in this line. This transgenic line with dose-dependent behavior, a desirable trait for subsequent suppressor analysis (see below), did not seem atypical because independent transgenic lines showed a very similar root meristem phenotype (data not shown) and hemizygous primary transformants with short roots showed a marked tendency for multicopy insertions.

Homozygous *RCH1-CLE19* roots progressively lose cells in the meristematic zone (Figures 1E and 1G), and this loss is also indicated by the formation of root hairs closer to the root tip. In many cases, the root meristem is eventually consumed, while this never happens in control roots (Figures 1D, 1F, and 1J). To substantiate that the phenotype of *RCH1-CLE19* roots was due to the overexpression of CLE19 protein, we replaced codon 3 of *CLE19* in the *RCH1-CLE19* construct with a stop codon, creating the *RCH1-CLE19stop* vector. Independent plants transformed with this vector all have a WT appearance (data not shown). We concluded that the *CLV3* homolog *CLE19* induces differentiation or represses cell division of meristematic cells when overexpressed in roots. The observed reduction of root meristem size is consistent with the hypothesis that CLE19 and likely other CLE family members locally activate endogenous CLV-like receptors involved in root meristem maintenance, although we cannot exclude at this point that other signaling pathways are activated by CLE protein overexpression in the root.

Overexpression of CLE19 Does Not Primarily Affect QC and Stem Cell Identity

A failure in root meristem maintenance can be caused by the loss of stem cell maintenance, by lack of QC activity or specification [8, 9], or by loss of division potential and/or more rapid differentiation of stem cell daughters. In the first case, primary defects in the QC region would be expected, while in the second case, meristem size would decrease before QC and stem cells show defects.

To assess whether QC specification and stem cell maintenance are rapidly affected in *RCH1-CLE19* transgenic plants, we introduced QC markers QC25 and QC184 [15] into these plants (Figures 1I and 1J; data not shown). *RCH1-CLE19* transgenic roots still express these markers 1 week after germination, when root meristem size is already significantly reduced compared to

WT (Figures 1H and 1I), and only upon complete differentiation of root meristem cells do they disappear (Figure 1J). One week after germination, no starch granules that mark differentiated columella cells could be detected in the columella stem cells of 73% (n = 26) of the *RCH1-CLE19* transgenic seedlings analyzed (Figures 1H and 1I, arrow), suggesting that stem cell status is maintained for a prolonged period.

The expression of both QC markers together with the maintenance of columella stem cells in *RCH1-CLE19* transgenic seedlings, at a stage when meristem size is already significantly decreased, indicates that overexpression of *CLE19* in the root meristem reduces meristem size without primarily interfering with QC specification and/or stem cell maintenance.

The CLE19-Induced Pathway Is Independent of SHR and SCR

In *short root* (*shr*) and *scarecrow* (*scr*) mutants, root growth ceases prematurely, as observed in *RCH1-CLE19* transgenic plants (Figures 1K and 1M; [16, 17]). SHR and SCR are both members of the GRAS family of putative transcription factors, and they are required for QC specification and stem cell maintenance [9, 18, 19]. In *scr* and *shr* mutants, the QC25 marker is never expressed and the columella initials differentiate [9]. Our observation that QC and stem cells are not primarily affected in *RCH1-CLE19* transgenic roots suggests that CLE19 interferes with meristem size independently or downstream of SHR and SCR.

To investigate whether CLE19 interferes downstream of SHR and SCR, we introduced *RCH1-CLE19* in *shr-1* and *scr-1* mutants. *RCH1-CLE19 shr-1* double homozygotes show additive phenotypes; the reduction in root meristem size occurs faster than in either single homozygote, as seen by the decreased number of meristematic cells (Figures 1K–1M, arrowhead) and the closer proximity of root hairs to the tip. As a measure for meristem size, we counted the number of cortex cells in a single file extending from the QC up to the first rapidly elongated cell of 6-day-old seedlings. *RCH1-CLE19 shr-1* contains an average of 1.8 ± 1.5 (n = 9) cortex cells per file in the meristem, while *RCH1-CLE19* contains 6.8 ± 0.4 (n = 4) and *shr-1* possesses 6.3 ± 0.4 (n = 5). Similar results were observed in *RCH1-CLE19 scr-1* double homozygotes (data not shown). Our data suggest that CLE19 acts independently of SHR and SCR; this finding is in line with the notion that CLE19 does not primarily interfere with the identity of the organizer and its activity in maintaining the surrounding stem cells. Rather, CLE19 seems to modulate the activity of the stem cell daughters that populate the meristem. This contrasts with the CLV pathway control of meristem size that is required for maintenance of stem cells by transcriptional repression of the putative homeodomain transcription factor *WUSCHEL* (*WUS*) in the organizing center of the SAM [1, 2]. Perhaps this mechanistic difference reflects that SAM stem cells are regulated as a population; root meristem stem cells are regulated at the single cell level, while the division potential of their daughters, i.e., root meristem size, is regulated at the population level.

Mutagenesis Screen for Suppressors of *RCH1-CLE19*

To find molecular components involved in the root meristem maintenance defect caused by overexpression of *CLE19*, an ethylmethane sulfonate (EMS) mutagenesis was performed in the *RCH1-CLE19* background to identify suppressors. A total of 8,100 mutagenized *RCH1-CLE19* M0 seeds were divided into 10 pools, and a minimum of 11,000 M2 seedlings were screened per pool for recovery of root length with high GFP (Figure 2A, arrow). Putative mutants were checked in the M3 generation for resegregation of the suppressor phenotype and were put in complementation groups by pairwise crossing. All recessive mutations that suppressed *RCH1-CLE19* resided at two novel loci and were named *suppressor of LLP1 1* and *2* (*sol1* and *sol2*). Four independent *sol1* alleles and two independent *sol2* alleles were obtained. We crossed all *RCH1-CLE19 sol1* and *RCH1-CLE19 sol2* alleles to *RCH1-CLE19*, and in both crosses, the F1 plants had short roots, indicating that *RCH1-CLE19* is still fully active in the suppressor background.

Both *RCH1-CLE19 sol1* and *RCH1-CLE19 sol2* completely suppress the root length and meristem defect seen in the *RCH1-CLE19* transgenic plants up to 1 week after germination, and *RCH1-CLE19 sol1* alleles maintain complete suppression (Figures 2B–2E, arrowheads, Figures 2F and 2G). In contrast, roots of both *RCH1-CLE19 sol2* alleles become shorter than WT 15 days postgermination (dpg), indicating loss of suppression (Figure 2F). We measured meristem size as before, and we observed no significant difference among *RCH1-CLE19 sol1* alleles and WT; however, all *RCH1-CLE19 sol2* alleles contain less meristem cells at 15 dpg (Figure 2G). These results suggest that *RCH1-CLE19 sol2* alleles are not complete suppressors of *RCH1-CLE19*.

Homozygous *sol1-3* and *sol2-1* alleles without the *RCH1-CLE19* construct did not show any differences in root length or in meristem size compared to control plants (data not shown) and hence conferred no root phenotype on their own.

sol2 Flowers Have Extra Carpels, Reminiscent of *clv* Mutant Defects

Terminal *RCH1-CLE19 sol2* flowers occasionally accumulate a central mass of carpeloid filaments with stigmatic tissue (Figure 3A), which may be accompanied by fasciation of the main stem (data not shown). Closer inspection revealed that 45% of early *RCH1-CLE19 sol2-2* flowers and 15% of *RCH1-CLE19 sol2-1* flowers contain extra carpels in the last whorl. The floral phenotypes of *RCH1-CLE19 sol2* cosegregated with the suppression phenotype (see the Supplemental Data available with this article online). *SOL2* was mapped to a region on the bottom arm of chromosome II (data not shown).

When the *RCH1-CLE19 sol2-1* allele was crossed to the Landsberg-*er* (L-*er*) ecotype for mapping purposes, we noticed that the penetrance of the floral phenotypes was higher in the F2 plants homozygous for *RCH1-CLE19 sol2-1*. Up to 80% of *RCH1-CLE19 sol2-1* flowers in L-*er* hybrids possessed extra carpels in the last whorl
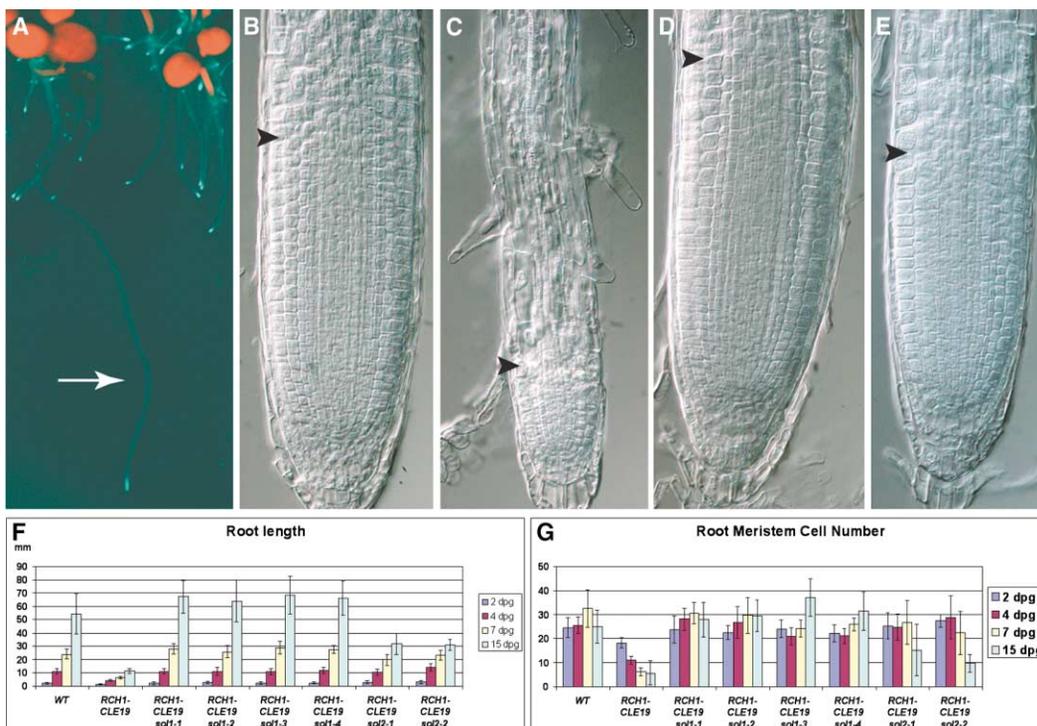
Figure 2. The *sol1* and *sol2* Mutants Suppress *RCH1-CLE19*-Induced Reduction of Root Meristem Size

(A) A suppressor mutant (arrow) has a long root with high GFP expression among *RCH1-CLE19* transgenic seedlings possessing short roots with high GFP.

(B–E) Nomarski images showing the root meristem boundary (arrowhead) of 1-week-old WT, *RCH1-CLE19*, *RCH1-CLE19 sol1*, and *RCH1-CLE19 sol2* roots, respectively.

(F and G) Root length (in mm) and root meristem cell number of WT, *RCH1-CLE19*, and the different *RCH1-CLE19 sol1* and *RCH1-CLE19 sol2* alleles. For root length, a minimum of 16 roots were measured per line, while 10 roots per line were used to determine the root meristem cell number for each time point (see the Supplemental Data). The bars indicate the standard deviation of the mean.

(3.4 ± 0.8 carpels per flower), which was never observed for *RCH1-CLE19* flowers in L-*er* hybrids (2 ± 0 carpels per flower; Figures 3C–3E). In addition, we again observed accumulation of carpeloid organs in some terminal flowers (Figure 3B). The higher penetrance of the *RCH1-CLE19 sol2* floral phenotype in a mixed background was not due to the *er* mutation, since *er* is linked to the *RCH1-CLE19* insertion and hence counterselected for (data not shown). In *sol2-1* outcrossed to Col-0 homozygotes without the *RCH1-CLE19* construct, 34% of the flowers had extra carpels in the last whorl, indicating that the floral phenotype is not dependent on *CLE19* overexpression.

The presence of extra carpels in the fourth whorl of

Figure 3. *sol2* Mutants Alter Flower Development

(A) Accumulation of carpeloid organs in terminal flowers of *RCH1-CLE19 sol2-1* transgenic plants.

(B) Accumulation of carpeloid organs in terminal flowers of homozygous *RCH1-CLE19 sol2* F2 plants after outcrossing to L-*er*.

(C and D) Carpels of homozygous *RCH1-CLE19* and *RCH1-CLE19 sol2* F2 plants after outcrossing to L-*er*.

(E) Average number of floral organs in each whorl of *RCH1-CLE19* and *RCH1-CLE19 sol2-1* F2 plants after outcrossing to L-*er*. Only the first ten flowers of any given plant were analyzed. The mean value and standard deviation of the mean of indicated floral organs is depicted. A total of 60 flowers from 6 *RCH1-CLE19* transgenic plants and 120 flowers from 12 *RCH1-CLE19 sol2-1* plants of the L-*er* hybrids were counted for each mean calculated.

sol2 flowers suggests that stem cells may accumulate in the flower meristem of these mutants, as observed in *clv* mutants. This observation is consistent with the hypothesis that *sol2* is affected in a CLV-type signaling pathway.

SOL1 Encodes a Putative Zn^{2+}-Carboxypeptidase

To investigate the molecular basis of the *sol1* mutations, we isolated the affected gene by map-based cloning. *sol1* mapped to a single locus on chromosome 1 between markers nga128 and nga111 (Figure 4A). Fine mapping located the gene in between bp 92082 of BAC F5H11 and bp 10734 of BAC F17M19 (Figure 4B).

Locus *At1g71696* in this region was predicted to encode a putative carboxypeptidase, and we analyzed this locus since the carboxypeptidase BRS1 had been linked to brassinolide signaling through the LRR-RLK BRI1 [20]. With the corresponding WT as control, we detected different mutations in the *At1g71696* gene for all four *sol1* alleles (Figure 4C).

We concluded that *SOL1* encodes a single-copy putative regulatory Zn^{2+}-carboxypeptidase showing high homology to conserved domains of animal carboxypeptidase D [21] and carboxypeptidase E (Figure 4E). SOL1 contains all the conserved residues present in these proteins: the triad H, E, H involved in Zn^{2+} binding, the R and Y involved in substrate binding, and the E involved in catalytic activity (Figures 4D and 4E, asterisks, squares, and circles, respectively). SOL1 is predicted to be a transmembrane protein with a small cytoplasmic tail (Figure 4D).

Four different *SOL1* cDNA variants (AJ555408, AJ555409, AJ555410, and AJ555411, Supplemental Data), which are the result of alternative splicing after exons 3 and 12, were detected in WT. Preliminary evidence suggests other splicing variants for either the WT and/or the *sol1* mutant alleles.

All mutations in *sol1* alleles are single base pair substitutions (Figure 4C). In *sol1-1*, the mutation is in an exon-intron boundary between exons 8 and 9 and yields either an unspliced variant predicted to result in a translational stop or an AA substitution in a conserved residue (G to S in AA 236; Supplemental Data). In *sol1-3*, the mutation is in the first exon-intron boundary and leads to multiple splicing variants that are all predicted to yield an early translational stop (Supplemental Data). *sol1-4* is predicted to yield an amino acid substitution in a conserved residue (G to D in amino acid 298), and in *sol1-2*, the mutation is predicted to result in a translational stop after 148 amino acids (Supplemental Data).

We isolated RNA from roots, shoots, leaves, flowers, siliques, and whole seedlings and performed Reverse Transcriptase (RT)-PCR reactions and detected two *SOL1* WT bands in all these tissues (Figure 4F). RT-PCR for *sol1* alleles showed that novel splicing variants are formed in *sol1-1* and *sol1-3*, consistent with the location of mutations in exon-intron boundaries (Figure 4F).

SOL1-homologous animal CPD and CPE have been shown to cleave terminal R and K residues and are involved in neuropeptide and prohormone processing [22]. It can be envisaged that SOL1 processes inactive CLE peptides with terminal R and K residues to a bioac-

tive form. Among *Arabidopsis* CLE members, there are different possible targets for SOL1 activity: terminal R or K residues after the CLE box (e.g., CLE19), internal R or K residues in the CLE proteins, or a conserved R in the CLE box of all CLE members [11]. The latter two classes of internal residues might be used for a two-step activation process, as described for animal neuropeptides [22]. Biochemical activity assays with SOL1 protein will be required to test this model.

It is noteworthy that *sol1* mutants without the *RCH1-CLE19* construct do not affect root growth. Currently, it is not certain whether any of the four *sol1* alleles is a null. For example, alternative splicing variants encoding proteins with residual activity could exist. In addition, alternative translational starts could be used, as the predicted SOL1 protein contains two methionine codons before the conserved residues but after the signal peptide (Figure 4D). Thus, there may be residual SOL1 carboxypeptidase activity, which could either process an endogenous ligand more efficiently than CLE19 or could process enough of an endogenous ligand with higher affinity to its receptor than CLE19. Such scenarios would explain why *sol1* has no *clv*-like phenotypes. We call to mind that *RCH1-CLE19* is dose dependent and that reduction of activity by 50% is sufficient to eliminate its ectopic activity. In comparison, flower phenotypes in *clv3* mutants are recessive or very slightly semidominant, indicating that their activity has to be reduced by more than 50% for obvious phenotypic consequences [14]. Another explanation for the lack of *clv* phenotypes may be redundancy with BRS1, whose overexpression can suppress *bri1* extracellular domain mutants. BRS1 has homology to yeast Kex1p and has also been proposed to act in ligand processing in the brassinosteroid signal transduction pathway [20]. Kex1p cuts the C-terminal amino acid from signaling peptide intermediates [23]. Thus, it is possible that even though BRS1 and SOL1 belong to structurally different classes of carboxypeptidases, they might be redundant at the functional level.

We present here three lines of evidence suggesting that a CLV-like pathway is involved in root meristem maintenance. First, overexpression of *CLE19* specifically in the root meristem causes defective root meristem maintenance, analogous (albeit mechanistically different) to the defective meristem maintenance conveyed by overexpression of CLV3 [6]. High levels of expression of CLV3 or CLE40 also reduce root meristem activity, suggesting that all these ligands are able to overactivate an endogenous CLV-like pathway [13]. Second, *sol2* contains extra carpels in the fourth whorl, reminiscent of the phenotypes of weak *clv* alleles (like *clv1-7*; [24]) and suggesting that CLV components may be shared between roots and shoots. Third, *SOL1* encodes a candidate processing enzyme for CLE-type ligands.

In *Arabidopsis*, there are more than 400 receptor-like kinases (RLK), but only in very few cases has a function been identified [25]. For the well-characterized *clv1* mutants, it has recently been reported that strong and intermediate alleles are dominant negative, while null mutants show only weak phenotypes. These findings suggest a possible role for other receptor(s) in the same
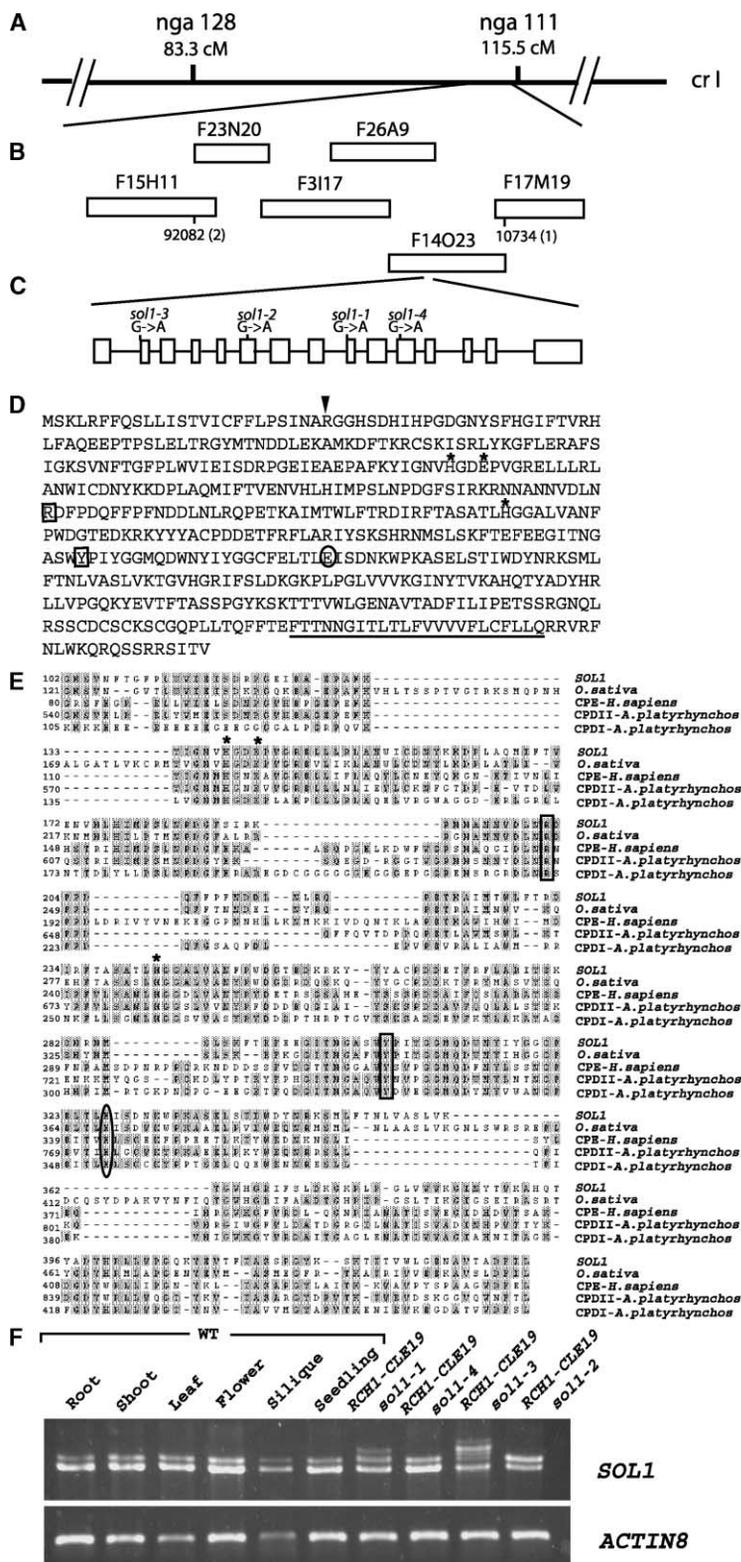
Figure 4. SOL1 Encodes a Putative Zn²⁺-Carboxypeptidase

(A) sol1 mutations map between markers nga128 and nga111.

(B) sol1 is located between BACs F15H11 and F17M19. The position and number of recombinants (in parenthesis) with the closest markers are shown below the corresponding BACs.

(C) Structure of SOL1: the white boxes represent exons (5′ and 3′ UTR not included). Nucleotide sequence changes are depicted for each allele.

(D) The SOL1 protein sequence from splicing variant AJ555408 that corresponds to the longest predicted protein. The predicted signal peptide cleavage site is marked with an arrowhead, and the putative transmembrane domain is underlined. The carboxypeptidase conserved residues are depicted as follows: the triad H, E, H involved in Zn²⁺ binding is depicted with an asterisk, the R and Y involved in substrate binding are depicted with a square, and the E responsible for the catalytic activity is depicted with a circle.

(E) Alignment of the carboxypeptidase conserved region from SOL1, Oriza sativa, the first and second domains of Anas platyrhynchos Carboxypeptidase D (CPD), and Homo sapiens Carboxypeptidase E (CPE). The conserved residues crucial for carboxypeptidase activity are depicted as in (D).

(F) RT-PCR reaction using total RNA from roots, shoots, leaves, flowers, siliques, and whole seedlings for WT plants and whole seedlings for sol1 alleles. Specific primers for SOL1 (32 cycles, upper panel) and ACTIN8 (23 cycles, lower panel) were used. For a description of splicing variants, see the Supplemental Data.

Panel D protein sequence:

MSKLRFFQSLLISTVICFFLPSINARGGHSDHIHPGDGNYSFHGIFTVRH
LFAQEEPTPSLELTRGYMTNDDLEKAMKDFTKRCSKISRLYKGFLERAFS
IGKSVNFTGFPLWVIEISDRPGEIEAEPAFKYIGNVHGDEPVGRELLLRL
ANWICDNYKKDPLAQMIFTVENVHLHIMPSLNPDGFSIRKRNNANNVDLN
RDFPDQFFPFNDDLNLRQPETKAIMTWLFTRDIRFTASATLHGGALVANF
PWDGTEDKRKYYYACPDDETFRFLARIYSKSHRNMSLSKFTEFEEGITNG
ASWYPIYGGMQDWNYIYGGCFELTIQISDNKWPKASELSTIWDYNRKSML
FTNLVASLVKTGVHGRIFSLDKGKPLPGLVVVKGINYTVKAHQTYADYHR
LLVPGQKYEVTFTASSPGYKSKTTTVWLGENAVTADFILIPETSSRGNQL
RSSCDCSCKSCGQPLLTQFFTEFTTNNGITLTLFVVVVFLCFLLQRRVRF
NLWKQRQSSRRSITV

process [26]. Cloning of sol2 will clarify if it encodes a root CLV1-type receptor. It is of note that our suppressor screen yielded several as yet uncharacterized mutants with unusual segregation ratios, and it can now be tested whether they represent dominant-negative alleles. In a reverse genetic approach, we identified CLV1-like receptors specifically expressed in the root meristem, but loss-of-function mutations in these genes revealed no phenotype, not even in double mutant combinations (data not shown). These results indicate redundancy

among LRR-RLKs in roots, and more investigation will be required to identify the critical receptors in a root CLV pathway.

References

1. Mayer, K.F.X., Schoof, H., Haecker, A., Lenhard, M., Jurgens, G., and Laux, T. (1998). Role of *WUSCHEL* in regulating stem cell fate in the *Arabidopsis* shoot meristem. Cell *95*, 805–815.

2. Schoof, H., Lenhard, M., Haecker, A., Mayer, K.F.X., Jurgens, G., and Laux, T. (2000). The stem cell population of *Arabidopsis* shoot meristems is maintained by a regulatory loop between *CLAVATA* and *WUSCHEL* genes. Cell *100*, 635–644.

3. Fletcher, J.C., Brand, U., Running, M.P., Simon, R., and Meyerowitz, E.M. (1999). Signaling of cell fate decisions by *CLAVATA3* in *Arabidopsis* shoot meristems. Science *266*, 605–614.

4. Trotochaud, A.E., Hao, T., Wu, G., Yang, Z., and Clark, S.E. (1999). The CLAVATA1 receptor-like kinase requires CLAVATA3 for its assembly into a signaling complex that includes KAPP and a Rho-related protein. Plant Cell *11*, 393–405.

5. Rojo, E., Sharma, V.K., Kovaleva, V., Raikhel, N.V., and Fletcher, J.C. (2002). CLV3 is localized to the extracellular space, where it activates the *Arabidopsis* CLAVATA stem cell signaling pathway. Plant Cell *14*, 969–977.

6. Brand, U., Fletcher, J.C., Hobe, M., Meyerowitz, E.M., and Simon, R. (2000). Dependence of stem cell fate in *Arabidopsis* on a feedback loop regulated by *CLV3* activity. Science *289*, 617–619.

7. Dolan, L., Janmaat, K., Willemsen, V., Linstead, P., Poethig, S., Roberts, K., and Scheres, B. (1993). Cellular organization of the *Arabidopsis thaliana* root. Development *119*, 71–84.

8. van den Berg, C., Willemsen, V., Hendriks, G., Weisbeek, P., and Scheres, B. (1997). Short-range control of cell differentiation in the *Arabidopsis* root meristem. Nature *390*, 287–289.

9. Sabatini, S., Heidstra, R., Wildwater, M., and Scheres, B. (2003). *SCARECROW* is involved in positioning the stem cell niche in the *Arabidopsis* root meristem. Genes Dev. *17*, 354–358.

10. van den Berg, C., Willemsen, V., Hage, W., Weisbeek, P., and Scheres, B. (1995). Cell fate in the *Arabidopsis* root meristem determined by directional signaling. Nature *378*, 62–65.

11. Cock, J.M., and McCormick, S. (2001). A large family of genes that share homology with *CLAVATA3*. Plant Physiol. *126*, 939–942.

12. Sharma, V.K., Ramirez, J., and Fletcher, J.C. (2003). The *Arabidopsis CLV3*-like (*CLE*) genes are expressed in diverse tissues and encode secreted proteins. Plant Mol. Biol. *51*, 415–425.

13. Hobe, M., Müller, R., Grünewald, M., Brand, U., and Simon, R. (2003). Loss of CLE40, a protein functionally equivalent to the stem cell restricting signal CLV3, enhances root waving in *Arabidopsis*. Dev Genes Evol (epub ahead of print).

14. Clark, S.E., Running, M.P., and Meyerowitz, E.M. (1995). *CLA-*

15. Sabatini, S., Beis, D., Wolkenfelt, H., Murfett, J., Guilfoyle, T., Malamy, J., Benfey, P., Leyser, O., Bechtold, N., Weisbeek, P., et al. (1999). An auxin-dependent distal organizer of pattern and polarity in the *Arabidopsis* root. Cell *99*, 463–472.

16. Benfey, P.N., Linstead, P.J., Roberts, K., Schieferlbein, J.W., Hauser, M.T., and Aeschbacher, R.A. (1993). Root development in *Arabidopsis*: four mutants with dramatically altered root morphogenesis. Development *119*, 57–70.

17. Scheres, B., Di Laurenzio, L., Willemsen, V., Hauser, M.T., Janmaat, K., Weisbeek, P., and Benfey, P.N. (1995). Mutations affecting the radial organization of the *Arabidopsis* root display specific defects throughout the embryonic axis. Development *121*, 53–62.

18. Helariutta, Y., Fukaki, H., Wysocka-Diller, J., Nakajima, K., Jung, J., Sena, G., Hauser, M.T., and Benfey, P. (2000). The *SHORT-ROOT* gene controls radial patterning of the *Arabidopsis* root through radial signaling. Cell *101*, 555–567.

19. Di Laurenzio, L., Wysocka-Diller, J., Malamy, J.E., Pysh, L., Helariutta, Y., Freshour, G., Hahn, M.G., Feldmann, K.A., and Benfey, P.N. (1996). The *SCARECROW* gene regulates an asymmetric cell division that is essential for generating the radial organization of the *Arabidopsis* root. Cell *86*, 423–433.

20. Li, J., Lease, K.A., Tax, F.E., and Walker, J.C. (2001). BRS1, a serine carboxypeptidase, regulates BRI1 signaling in *Arabidopsis thaliana*. Proc. Natl. Acad. Sci. USA *98*, 5916–5921.

21. Aloy, P., Companys, V., Vendrell, J., Aviles, F.X., Fricker, L.D., Coll, M., and Gomis-Rüth, F.X. (2001). The crystal structure of the inhibitor-complexed carboxypeptidase D domain II and the modeling of regulatory carboxypeptidases. J. Biol. Chem. *11*, 16177–16184.

22. Nillni, E.A., Xie, W., Mulcahy, L., Sanchez, V.C., and Wetsel, W.C. (2002). Deficiencies in Pro-thyrotropin-releasing hormone processing and abnormalities in thermoregulation in *Cpe^{fat/fat}* mice. J. Biol. Chem. *277*, 48587–48595.

23. Domchowska, A., Dignard, D., Henning, D., Thomas, D.Y., and Bussey, H. (1987). Yeast KEX1 gene encodes a putative protease with a carboxypeptidase B-like function involved in killer toxin and α-factor precursor processing. Cell *50*, 573–584.

24. Clark, S.E., Running, M.P., and Meyerowitz, E.M. (1993). *CLAVATA1*, a regulator of meristem and flower development in *Arabidopsis*. Development *119*, 397–418.

25. Shiu, S.H., and Bleecker, A.B. (2001). Receptor-like kinases from *Arabidopsis* form a monophyletic gene family related to animal receptor kinases. Proc. Natl. Acad. Sci. USA *98*, 10763–10768.

26. Diévart, A., Dalal, M., Tax, F.E., Lacey, A.D., Huttly, A., Li, J., and Clark, S.E. (2003). *CLAVATA1* dominant-negative alleles reveal functional overlap between multiple receptor kinases that regulate meristem and organ development. Plant Cell *15*, 1198–1211.

VATA3 is a specific regulator of shoot and floral meristem development affecting the same process as *CLAVATA1*. Development *121*, 2057–2067.